Polymer Chemistry

Accepted Manuscript

ROYAL SOCIETY OF CHEMISTRY

www.rsc.org/polymers

Toward a Tunable Synthetic [FeFe] Hydrogenase Mimic: Single-chain Nanoparticles Functionalized With a Single Diiron Cluster

C. A. Tooley,[a] S. Pazicni,[a]* and E. B. Berda[a,b]*

a. University of New Hampshire, Department of Chemistry, 23 Academic Way, Durham, NH 03824.

b. University of New Hampshire, Materials Science Program, 23 Academic Way, Durham, NH 03824.

Electronic Supplementary Information (ESI) available. See DOI.

We report two novel "clickable" [(μ-$S_2C_2H_4NR$)$Fe_2(CO)_6$] complexes and their incorporation into single-chain nanoparticles. Variations in the characteristic iron-carbonyl stretching bands caused by the polymer scaffolds confirmed changes in symmetry and electronics of the complexes. This represents the first SCNP-based models of a metalloenzyme bearing a single, bioinspired active site.

Movement towards clean and sustainable energy sources has led to an interest in molecular hydrogen production for fuel.[1] Developing catalysts for producing H_2 under very mild conditions has inspired the design and synthesis of model complexes of hydrogenases, a class of metalloenzymes found in bacteria and select archaea that catalyze both H_2 oxidation and production. The hydrogenases are categorized according to the metals that compose the active site: [NiFe], [FeFe], and [Fe].[2, 3] Of these hydrogenases, [FeFe] hydrogenase (Fe_2-H_2ase) is most efficient at H_2 production at pH = 7 and under mild reduction potentials (-0.4 V vs. NHE).[4-7] The active site of Fe_2-H_2ase (**Fig. 1**) is quite unique among metalloenzymes: an azadithiolate-bridged Fe_2S_2 unit linked to a Fe_4S_4 cubane by an endogenous cysteine thiolate moiety.[8] Catalytically competent model complexes based on the Fe_2S_2 subunit of Fe_2-H_2ase have been reported; however, these small molecule catalysts possess reduction potentials ~1 V more negative than the native enzyme.[9] The hydrophobic pocket, in which the Fe_2-H_2ase active site is located, must be crucial for tuning the properties of the Fe_2-H_2ase active site.

While the primary coordination sphere fundamentally affects the reactivity of a metalloenzyme active site, secondary coordination sphere effects also play a role in tuning reactivity.[10] The secondary coordination sphere of synthetic metal catalysts can be altered through the use of ligand substituents. However, a ligand's small size results in an environment that does not completely surround the metal center and its first coordination sphere.[11] Metalloenzymes resolve this issue through a well-defined polypeptide tertiary structure, which forces the metalloenzyme's active site into an entatic state, enhancing reactivity via an energized ground state.[12] We hypothesize that a macromolecular environment such as that provided in the enzyme is necessary for realizing the full catalytic capacity of complexes that model active sites of metalloenzymes like Fe_2-H_2ase.

Recent work supports this conjecture. Hayashi *et al.*, covalently bound a $Fe_2(CO)_6$ Fe_2-H_2ase model complex to CXXC-containing peptides derived from two different cytochromes; they demonstrated that the catalytic activity of the $Fe_2(CO)_6$ was enhanced in these peptide environments.[13, 14] Successful binding of the $Fe_2(CO)_6$ complex to cytochrome scaffolds was determined using IR spectroscopy to observe changes in the CO stretching energies of the $Fe_2(CO)_6$ unit, which occur between 1800-2200 cm^{-1}. In a subsequent investigation, catalytic activity of the $Fe_2(CO)_6$ complex was further enhanced when it was embedded within the protein nitrobindin, whose *β*-barrel fold provides a hydrophobic environment analogous to the native enzyme.[15]

Covalently linking Fe_2-H_2ase model complexes to synthetic polymer scaffolds permits more chemically diverse environments, relative to native peptide scaffolds, which we believe provides an avenue to fine tune reactivity. Yu et al. incorporated a Fe_2-$H_z$ase model complex into a synthetic hydrophobic dendrimer.[16] Interestingly, catalytic turnover numbers (TONs) were as high as 22,200 in aqueous media. Clearly, the macromolecular environment was critical for observing catalytic enhancement and this work represents an enormous step forward. However, the stepwise nature of dendrimer synthesis is typically tedious.[17] A more facile approach is single-chain nanoparticles (SCNPs), a method currently popular for creating architecturally defined nanostructures in the same size regime as dendrimers.

Numerous examples of exploiting SCNPs to enhance activity of synthetic catalysts have been reported. Huerta *et al.* reported a water-soluble methacrylate-based random copolymer possessing structural benzene-1,3,5-tricarboxamide (BTA) and L-proline organocatalytic units.[18] Catalytic aqueous aldol condensation was observed in this system when the polymer was folded, presumably because the hydrophobic (BTA) units formed a flexible compartment containing L-proline. Artar *et al.* prepared polymer chains possessing diphenylphosphinostyrene (SDP) units to bind $RuCl_2(PPh_3)_3$ through ligand substitution, which would simultaneously provide pseudocross-links.[19] Terashima *et al.* previously reported hydrogenation of cyclohexanone also using these Ru(II)-SDP SCNPs.[20] Sanchez-Sanchez *et al.* demonstrated substrate selectivity when Cu(II) catalysts were complexed to a methyl methacrylate-based SCNPs relative to free Cu(II) catalyst,[21] and reported SCNPs with polymerase-like activity in a more recent contribution.[22] Perez-Baena *et al.* were able to use $B(C_6F_5)_3$-functionalized SCNPS to catalyze the conversion of an α-diketone to a silyl-protected 1,2-diol with TOFs higher than the free-catalyst.[23] Willenbacher *et al.* prepared a polystyrene-based random polymer adorned with triphenylphosphine moieties that complexed Pd(II) catalysts, simultaneously folding the polymer into a SCNP.[24] This SCNP-bound Pd(II) complex displayed activity for performing Sonagashira cross-coupling reactions. Mavila *et al.* prepared poly(COD) by ROMP and folded the polymer by complexing Rh(I).[25] Subsequent catalytic studies using Rh(I) and Ir(I) as cross-linkers and catalysts revealed activities that were distinct from free catalyst.[26] While these elegant steps toward biomimetic catalysis have delineated some of the basic structure property

elements required for enzymatic activity in synthetic systems, no current studies examine incorporation of metalloenzyme-inspired catalysts into SCNPs.

We report here a new site-specific method to covalently bind a single transition metal complex based on the active site of Fe_2-H_2ase to various polymer chains. Our work includes a hydrophobic photocross-linkable scaffold, which can envelope the model complex in a SCNP, affording a tunable environment more similar to that of the native enzyme than competing model systems. While imparting SCNPs with enzyme-mimetic qualities by the addition of organo– and transition metal catalysts has become a growing area of research, we believe the systems reported here are the first completely synthetic models of a true metalloenzyme using SCNPs.

Two novel dithiolato diiron(I) hexacarbonyl model complexes based on the active site of Fe_2-H_2ase, [(μ-$S_2C_2H_4NR)Fe_2(CO)_6$], were synthesized with R = allyl (**1**) or propargyl (**2**) pendant functional groups (**Scheme 1**). This pendant functionality was bound to the thiol end-groups of polymer chains through thiol-ene/thiol-yne click reactions (**Scheme 2**). The [(μ-$S_2C_2H_4NR)Fe_2(CO)_6$] complexes **1** and **2** were prepared from (μ-dithiolato)diiron(I) hexacarbonyl, [(μ-S_2)$Fe_2(CO)_6$] following a modified procedure by Stanley *et al*.[27] Treatment of [(μ-S_2)$Fe_2(CO)_6$] with $LiEt_2BH$ affords [(μ-$SH)_2Fe_2(CO)_6$] *in situ* following acidic work-up. The bridging thiolato groups of [(μ-$SH)_2Fe_2(CO)_6$] were then alkylated with allyl- and propargylaminomethylation reagents to yield μ-allylazadithiolatodiiron(I) hexacarbonyl, [(μ-aadt)$Fe_2(CO)_6$] (**1**), and μ-propargylazadithiolatordiiron(I) hexacarbonyl, (μ-padt)$Fe_2(CO)_6$] (**2**), respectively. Crystals of both **1** and **2** were grown from hexanes and X-ray diffraction revealed C_{2v} symmetry in both complexes (**Fig. 2**). Given the identical ligand fields of **1** and **2**, it was unsurprising that we observed iron-bound CO stretches at similar energies for both complexes (**Fig**. **S1** and **fig. S2**). We also observed similar reduction potentials at –1.35 V vs. Fc/Fc^+ in acetonitrile for the two complexes (**Fig. S3** and **Fig. S4**), which are also similar to the reduction potential of the azadithiolate complex (-1.58 V vs. Fc/Fc^+).[28]

Polymer backbones were prepared using RAFT as it is amenable to many types of monomers and the RAFT agent chain-end provides a scaffold for attaching the cluster.[29-32] The diverse library of available monomers allowed us to investigate the effects of the various polymers on the click chemistry we employed to attach the Fe_2-H_2ase model complexes. Trithiocarbonate-based chain transfer end-groups were converted to a thiol through aminolysis with cyclohexylamine,[32] which resulted in white precipitated polymers (except for the polymer possessing anthracene repeat units). The polymer chains were then bound to an equivalent of the [(μ-$S_2C_2H_4NR)Fe_2(CO)_6$] complexes using thiol-ene/thiol-yne click chemistry in the presence of a photoinitiator (2,2'-dimethoxy-2-phenylacetophenone) (**Scheme 2**); the resulting pale red polymers were precipitated to

remove unreacted [(μ-$S_2C_2H_4NR$)$Fe_2(CO)_6$]. The polymer-bound Fe_2-H_2ase model complexes were then dissolved and dialyzed against THF to remove residual unreacted diiron cluster before a final precipitation.

SCNP formation experiments were performed under dilute conditions (0.5 mg/mL). We used UV-Vis absorbance spectroscopy to monitor the disappearance of anthracene absorbance bands between 300 and 400 nm and determine the length of time required to dimerize the anthracene repeat units (105 minutes). Aliquots from these UV-Vis absorbance experiments were analyzed by SEC. The chromatograms show that as the sample was irradiated with light centered at 350 nm in THF, intrachain folding occurred because the retention time increased by approximately one minute (**Fig. 4**). The small population of interchain-coupled polymer in our sample alsoe appeared to collapse. This increase in maximum retention time increase was reproducible and statistically significant (**SI: Section V**). The intrachain collapse of this system was further corroborated by viscometric data that indicate a decrease in intrinsic viscosity (η) upon irradiation because of the decrease in size of the polymer (**Table 1**). Further, a decrease in the viscometric radius ($R\eta$) of the system was also observed. It is important to note the difference in collapse data between polymer (**P1** and **SCNP1**) and polymer-bound complex **1** (**P2** and **SCNP2**) outlined in **Table 1**. This represents the first example of a SCNP possessing a single naturally inspired metal active site.

We isolated the SCNPs possessing complex **1** and characterized the sample by IR spectroscopy (**Fig. 5**). Despite the limited absorbance due to low concentration of polymer-bound complex **1**, we still observed small changes in the shape and energy of the iron-bound CO stretching energies. We do not anticipate much ligand dissociation from the irradiation with UV light because the native enzyme only dissociates an extra CO ligand below 180 K.[38] These changes suggest that a change in the polymer conformation (collapsing from from a random coil to a folded structure) affects the symmetry or electronics of complex **1**.

In summary, we report the first synthetic model of Fe_2-H_2ase that uses polymer chains to simulate the secondary coordination sphere interactions afforded to the active site by the native polypeptide. In doing so, we developed a novel method for covalently binding a single transition metal complex per linear polymer chain using photoinitiated thiol-ene/thiol-yne click chemistry. The presence of distinct iron-bound CO stretching bands occurring between 1800-2200 cm^{-1} in the IR spectrum of our polymer-bound [(μ-$S_2C_2H_4NR$)$Fe_2(CO)_6$] complexes demonstrated that the Fe_2-H_2ase model complexes were not compromised neither by this chemistry, nor the methods used to purify any of the polymer-bound systems. SCNPs were prepared from the polymer-bound complex **1** and confirmed by the SEC and viscometric data. IR spectroscopy revealed changes in the iron-bound CO stretching bands upon intrachain polymer collapse. This observation suggests that the change in

macromolecular conformation causes electronic changes in the complex **1**. We are currently investigating the effects of polymer conformation on catalytic activity of the [(μ-$S_2C_2H_4NR$)$Fe_2(CO)_6$] complexes.

The molecular weights used in this study preclude the use of NMR spectroscopy to determine the presence of Fe_2-H_2ase model complexes. FTIR spectroscopy proved useful because it is highly sensitive and provides very high signal-to-noise ratio. The presence of [(μ-$S_2C_2H_4NR$)$Fe_2(CO)_6$] in the polymers can be determined at high scans (minimum 1000) because of the distinct, albeit weak, signals at 1800-2200 cm^{-1} attributed to the CO ligands of [(μ-$S_2C_2H_4NR$)$Fe_2(CO)_6$] (**Fig. 3** and **Fig. S25-S28**). These IR spectra reveal changes in the carbonyl bands both in energy and band shape when [(μ-$S_2C_2H_4NR$)$Fe_2(CO)_6$] is bound to the polymer. This indicates there are distortions in the symmetry and electronics of [(μ-$S_2C_2H_4NR$)$Fe_2(CO)_6$] due to the presence of the polymer backbone. Distortions in the shape of the iron-bound CO bands can be attributed to a lack of well-defined structure in the macromolecular scaffold. Hence there is a clear difference in the shapes of the iron-bound CO stretches in our polymer-bound Fe_2-H_2ase model complex IR spectra when compared to those reported by Hayashi *et al*. This difference arises because the peptide-bound Fe_2-H_2ase model complexes are presumably in a more uniformly structured environment.[13, 15, 33]

While the second coordination spheres of complexes **1** and **2** appear to have been affected by simply attaching polymer scaffolds, we sought to more rigidly control the architecture of the polymer chain to simulate the environment of the native enzyme. To accomplish this, we prepared SCNPs from polymer-bound complex **1** by photoinduced intrachain folding. We prepared a methyl methacrylate-based copolymer possessing pendant anthracene crosslinking agent (22% relative to methyl methacrylate) (**P1, Scheme 2**; **Fig. S5**). Upon irradiation (λ_{max} = 350 nm) under dilute conditions, intrachain folding of this system occurs through [4πs+4πs] cycloadditions.[34-36] However, we found that subsequent aminolysis of the trithiocarbonate-based chain transfer end-group of this polymer (and, more general, those containing terminal methyl methacrylate repeating units) resulted in a thiolactone,[37] which was unreactive toward the click chemistry for attaching the [(μ-$S_2C_2H_4NR$)$Fe_2(CO)_6$] complexes. We therefore performed a gradient copolymerization with styrene to separate the end-group from methyl methacrylate repeat units (**P1**); this permitted successful binding of the complex **1** (**P2**). We characterized **P1** and **P2** using SEC (**Fig. 4; Table S1, Fig. S22-S23**). The MALS trace for **P2** displayed some shouldering at shorter retention times indicating the presence of some interchain coupling. However, the more uniform UV SEC trace for **P2** suggests that the shoulder in the MALS trace results from species of relatively low concentration. A control experiment involved SEC analysis of the aminolyzed polymer chain after bubbling compressed air into solution. The trace is identical to the parent polymer bearing a CTA end-group, which indicates that interchain coupling by disulfide formation was not occurring (**Fig. S6**).

SCNP formation experiments were performed under dilute conditions (0.5 mg/mL). We used UV-Vis absorbance spectroscopy to monitor the disappearance of anthracene absorbance bands between 300 and 400 nm and determine the length of time required to dimerize the anthracene repeat units (105 minutes). Aliquots from these UV-Vis absorbance experiments were analyzed by SEC. The chromatograms show that as the sample was irradiated with light centered at 350 nm in THF, intrachain folding occurred because the retention time increased by approximately one minute (**Fig. 4**). The small population of interchain-coupled polymer in our sample alsoe appeared to collapse. This increase in maximum retention time increase was reproducible and statistically significant (**SI: Section V**). The intrachain collapse of this system was further corroborated by viscometric data that indicate a decrease in intrinsic viscosity (η) upon irradiation because of the decrease in size of the polymer (**Table 1**). Further, a decrease in the viscometric radius (Rη) of the system was also observed. It is important to note the difference in collapse data between polymer (**P1** and **SCNP1**) and polymer-bound complex **1** (**P2** and **SCNP2**) outlined in **Table 1**. This represents the first example of a SCNP possessing a single naturally inspired metal active site.

We isolated the SCNPs possessing complex **1** and characterized the sample by IR spectroscopy (**Fig. 5**). Despite the limited absorbance due to low concentration of polymer-bound complex **1**, we still observed small changes in the shape and energy of the iron-bound CO stretching energies. We do not anticipate much ligand dissociation from the irradiation with UV light because the native enzyme only dissociates an extra CO ligand below 180 K.[38] These changes suggest that a change in the polymer conformation (collapsing from from a random coil to a folded structure) affects the symmetry or electronics of complex **1**.

In summary, we report the first synthetic model of Fe_2-H_2ase that uses polymer chains to simulate the secondary coordination sphere interactions afforded to the active site by the native polypeptide. In doing so, we developed a novel method for covalently binding a single transition metal complex per linear polymer chain using photoinitiated thiol-ene/thiol-yne click chemistry. The presence of distinct iron-bound CO stretching bands occurring between 1800-2200 cm^{-1} in the IR spectrum of our polymer-bound [(μ-$S_2C_2H_4NR$)$Fe_2(CO)_6$] complexes demonstrated that the Fe_2-H_2ase model complexes were not compromised neither by this chemistry, nor the methods used to purify any of the polymer-bound systems. SCNPs were prepared from the polymer-bound complex **1** and confirmed by the SEC and viscometric data. IR spectroscopy revealed changes in the iron-bound CO stretching bands upon intrachain polymer collapse. This observation suggests that the change in macromolecular conformation causes electronic changes in the complex **1**. We are currently investigating the effects of polymer conformation on catalytic activity of the [(μ-$S_2C_2H_4NR$)$Fe_2(CO)_6$] complexes.

Acknowledgements

We graciously acknowledge the University of New Hampshire for financial support, as well as the Army Research Office for support through award W911NF-14-1-0177. We also thank Jon Briggs for solving the reported crystal structures. We thank Prof. Todd Emrick and Rachel Letteri for assistance in acquiring PNIPAM SEC data through the financial support through The Materials Research Facilities Network (MRFN) supplement to the NSF-supported UMass MRSEC on Polymers (NSF-DMR-0820506).

Notes and References

†The dn/dc values are based on the parent polymer. See **Table S1** of SI for experimental and discussion.

1. T. R. Cook, D. K. Dogutan, S. Y. Reece, Y. Surendranath, T. S. Teets and D. G. Nocera, *Chem. Rev.*, 2010, **110**, 6474-6502.
2. P. M. Vignais, B. Billoud and J. Meyer, *FEMS Microbiol. Rev.*, 2001, **25**, 455-501.
3. R. K. Thauer, A.-K. Kaster, M. Goenrich, M. Schick, T. Hiromoto and S. Shima, *Ann. Rev. of Biochem.*, 2010, **79**, 507-536.
4. R. Cammack, *Nature*, 1999, **397**, 214-215.
5. E. C. Hatchikian, N. Forget, V. M. Fernandez, R. Williams and R. Cammack, *Eur. J. of Biochem.*, 1992, **209**, 357-365.
6. M. Frey, *ChemBioChem*, 2002, **3**, 153-160.
7. W. Lubitz, H. Ogata, O. Rüdiger and E. Reijerse, *Chem. Rev.*, 2014, **114**, 4081-4148.
8. T. B. Rauchfuss, *Acc. of Chem. Res.*, 2015, **48**, 2107-2116.
9. Z. Yu, M. Wang, P. Li, W. Dong, F. Wang and L. Sun, *Dalt. Trans.*, 2008, **18**, 2400-2406.

10. D. Balcells, P. Moles, J. D. Blakemore, C. Raynaud, G. W. Brudvig, R. H. Crabtree and O. Eisenstein, *Dalt. Trans.*, 2009, **30**, 5989-6000.
11. J. Yang, B. Gabriele, S. Belvedere, Y. Huang and R. Breslow, *J. Org. Chem.*, 2002, **67**, 5057-5067.
12. R. J. P. Williams, *Eur. J. of Biochem.*, 1995, **234**, 363-381.
13. Y. Sano, A. Onoda and T. Hayashi, *Chem. Comm.*, 2011, **47**, 8229-8231.
14. Y. Sano, A. Onoda and T. Hayashi, *J. Inorg. Biochem.*, 2012, **108**, 159-162.
15. A. Onoda, Y. Kihara, K. Fukumoto, Y. Sano and T. Hayashi, *ACS Catal.*, 2014, **4**, 2645-2648.
16. T. Yu, Y. Zeng, J. Chen, Y.-Y. Li, G. Yang and Y. Li, *Angew. Chem. Int. Ed.*, 2013, **52**, 5631-5635.
17. A.-M. Caminade, D. Yan and D. K. Smith, *Chem. Soc. Rev.*, 2015, **44**, 3870-3873.
18. E. Huerta, P. J. Stals, E. W. Meijer and A. R. Palmans, *Angew. Chem. Int. Ed.*, 2013, **52**, 2906-2910.
19. M. Artar, T. Terashima, M. Sawamoto, E. W. Meijer and A. R. A. Palmans, *J. of Polym. Sci. A Polym. Chem.*, 2014, **52**, 12-20.
20. T. Terashima, T. Mes, T. F. A. De Greef, M. A. J. Gillissen, P. Besenius, A. R. A. Palmans and E. W. Meijer, *J. Am. Chem. Soc.*, 2011, **133**, 4742-4745.
21. A. Sanchez-Sanchez, A. Arbe, J. Colmenero and J. A. Pomposo, *ACS Macro Lett.*, 2014, **3**, 439-443.
22. A. Sanchez-Sanchez, A. Arbe, J. Kohlbrecher, J. Colmenero and J. A. Pomposo, *Macromol. Rapid Commun.*, 2015, DOI: 10.1002/marc.201500252, ahead of print.
23. I. Perez-Baena, F. Barroso-Bujans, U. Gasser, A. Arbe, A. J. Moreno, J. Colmenero and J. A. Pomposo, *ACS Macro Lett.*, 2013, **2**, 775-779.
24. J. Willenbacher, O. Altintas, V. Trouillet, N. Knofel, M. J. Monteiro, P. W. Roesky and C. Barner-Kowollik, *Polym. Chem.*, 2015, **6**, 4358-4365.
25. S. Mavila, C. E. Diesendruck, S. Linde, L. Amir, R. Shikler and N. G. Lemcoff, *Angew. Chem. Int. Ed.*, 2013, **52**, 5767-5770.
26. S. Mavila, I. Rozenberg and N. G. Lemcoff, *Chem. Sci.*, 2014, **5**, 4196-4203.
27. J. L. Stanley, T. B. Rauchfuss and S. R. Wilson, *Organometallics*, 2007, **26**, 1907-1911.
28. M. Bourrez, R. Steinmetz and F. Gloaguen, *Inorg. Chem.*, 2014, **53**, 10667-10673.
29. G. Moad, E. Rizzardo and S. H. Thang, *Chem. Asian J.*, 2013, **8**, 1634-1644.
30. S. Meiliana, S. H. Brian and P. Sébastien, in *Progress in Controlled Radical Polymerization: Materials and Applications*, American Chemical Society, 2012, vol. 1101, ch. 2, pp. 13-25.

31. G. Moad, E. Rizzardo and S. H. Thang, *Polymer*, 2008, **49**, 1079-1131.

32. H. Willcock and R. K. O'Reilly, *Polym. Chem.*, 2010, **1**, 149-157.

33. Y. Sano, A. Onoda and T. Hayashi, *J. Inorg. Biochem.*, 2012, **108**, 159-162.

34. P. G. Frank, B. T. Tuten, A. Prasher, D. Chao and E. B. Berda, *Macromol. Rapid Comm.*, 2014, **35**, 249-253.

35. H. D. Becker, *Chem. Rev.*, 1993, **93**, 145-172.

36. W. Chen, J.-Y. Wang, W. Zhao, L. Li, X. Wei, A. C. Balazs, K. Matyjaszewski and T. P. Russell, *J. Am. Chem. Soc.*, 2011, **133**, 17217-17224.

37. J. Xu, J. He, D. Fan, X. Wang and Y. Yang, *Macromolecules*, 2006, **39**, 8616-8624.

38. Z. Chen, B. J. Lemon, S. Huang, D. J. Swartz, J. W. Peters and K. A. Bagley, *Biochemistry*, 2002, **41**, 2036-2043.

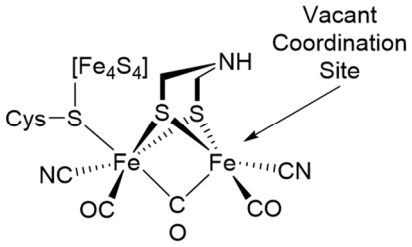

Figure 1. Schematic of the Fe_2-H_2ase active site. H^+ are proposed to bind to the vacant coordination site through oxidative addition, thereby initiating a catalytic cycle that produces H_2.

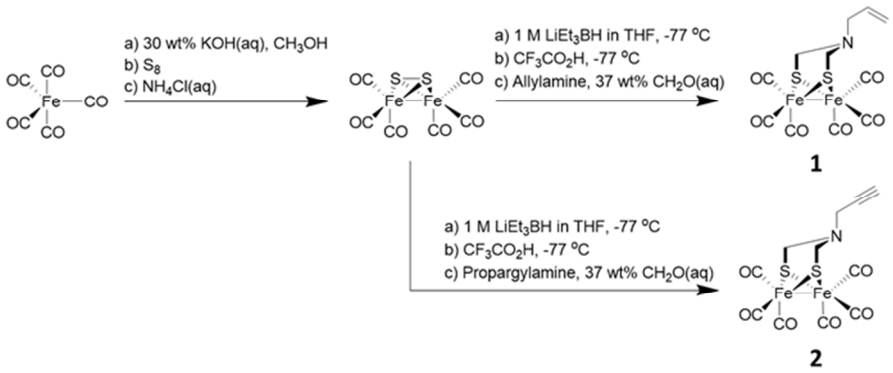

Scheme 1. Synthetic routes to the aadt (**1**) and padt (**2**) diiron hexacarbonyl cluster complexes.

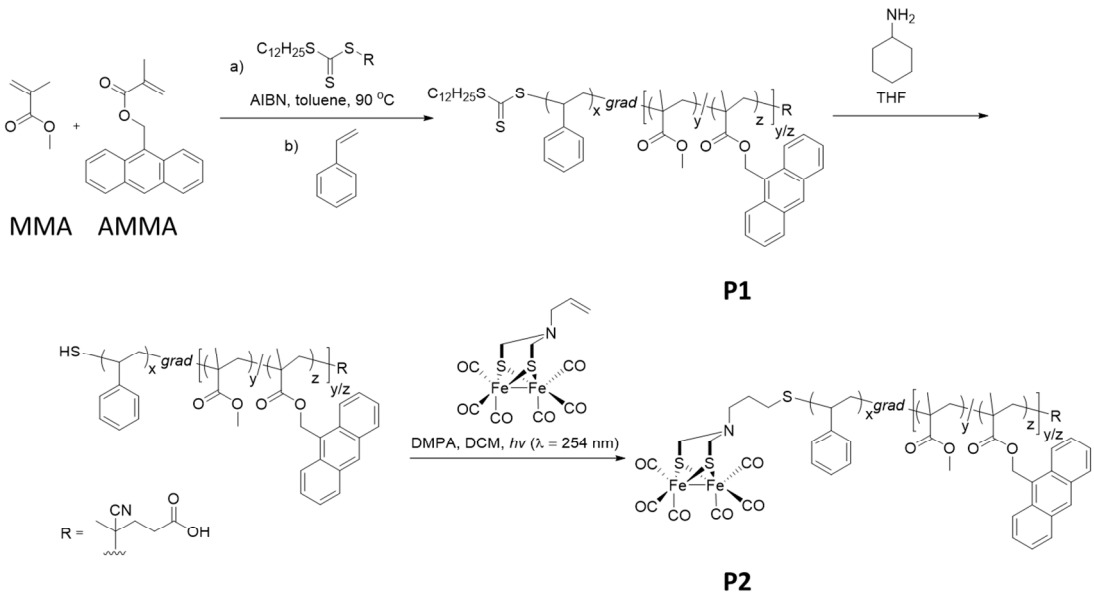

Scheme 2. Representative synthesis of a polymer-bound Fe_2-H_2ase model complex (**P2**). Here, complex **1** is covalently bound to a MMA/AMMA copolymer (**P2**).

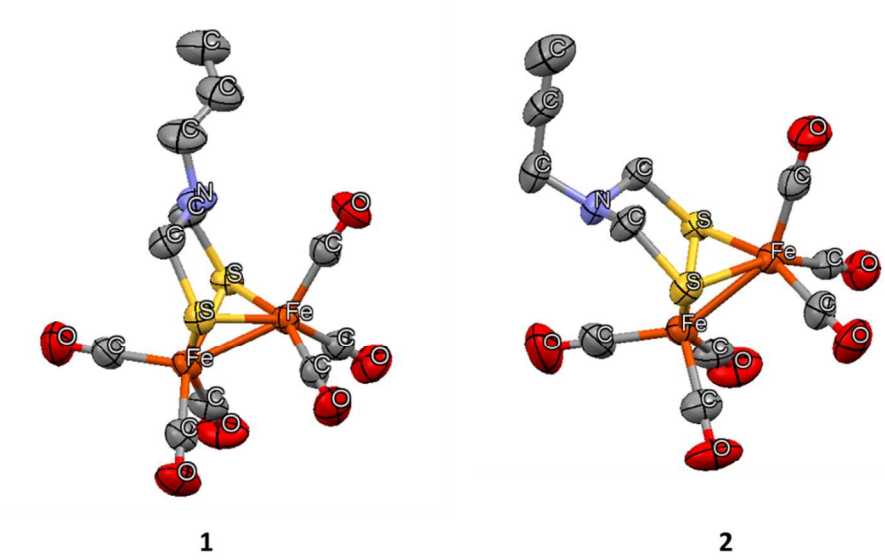

1 2

Figure 2. X-ray crystal structures of the aadt (**1**) and padt-bridged (**2**) diiron hexacarbonyl complexes.

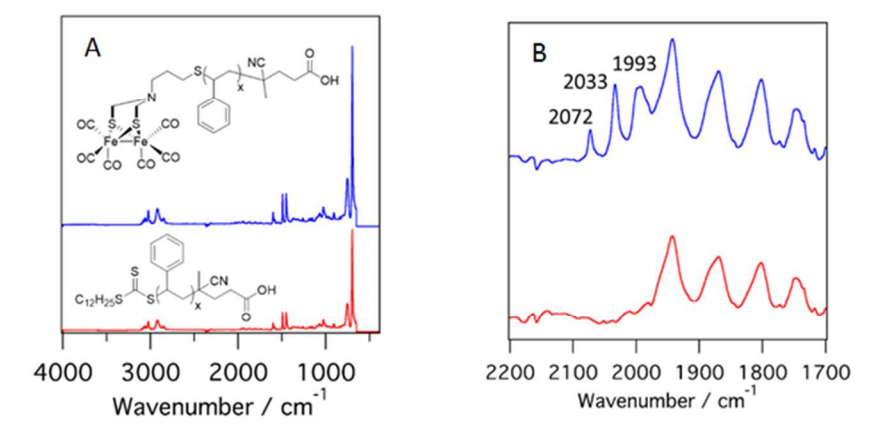

Figure 3. A) Full IR spectrum of polymer (red) and polymer-bound complex **1** (blue). B) Region of the spectrum corresponding to the energies of the iron-bound CO stretches. For these representative data, polystyrene was used as the polymer scaffold. See **fig. S27** and **fig. 28** for polymer-bound complex **2**.

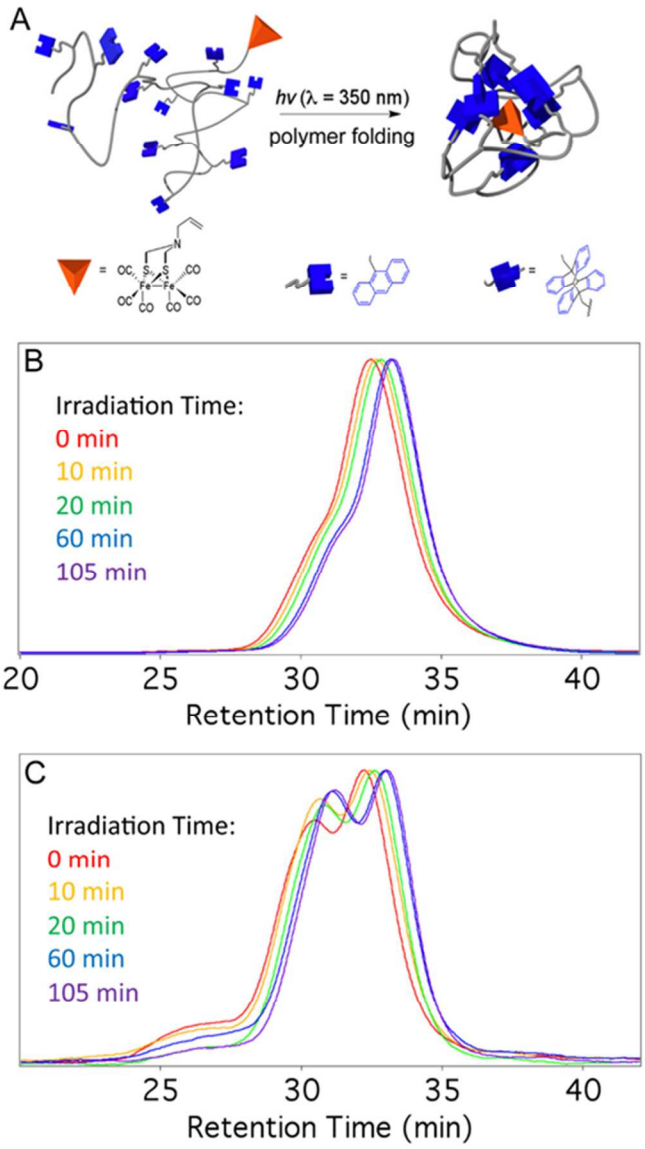

Figure 4. A) Schematic representation of polymer-bound complex **1** (**P2**) folding into a SCNP. B) UV SEC trace of **SCNP2** formation. C) MALS SEC trace of **SCNP2** formation.

Table 1. Comparison of SEC data for the MMA/AMMA copolymer before (**P1**) and after irradiation (**SCNP1**) to polymer-bound complex **1** before (**P2**) and after irradiation (**SCNP2**). Both systems were irradiated with λ_{max} = 350 nm radiation for 105 min.

	M_w (kDa)	M_n (kDa)	PDI	dn/dc (mL/g)	Rη (nm)	η (mL/g)
P1	35.4	32.8	1.08	0.135	3.69	9.79
SCNP1	31.0	28.6	1.08	0.134	2.92	5.64
P2	35.6	34.0	1.05	0.135†	3.65	9.13
SCNP2	31.7	30.3	1.05	0.134†	3.10	6.27

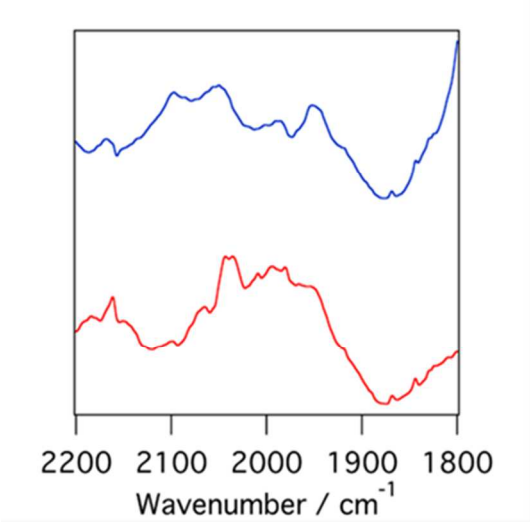

Figure 5. IR spectra of. polymer-bound complex **1** before (**P2**, red) and after irradiation (**SCNP2**, blue) with λ_{max} = 350 radiation for 105 min. For clarity, we show only the region of the spectrum corresponding to the energies of the iron-bound CO stretches. See **Fig. S7** for the full IR spectrum.

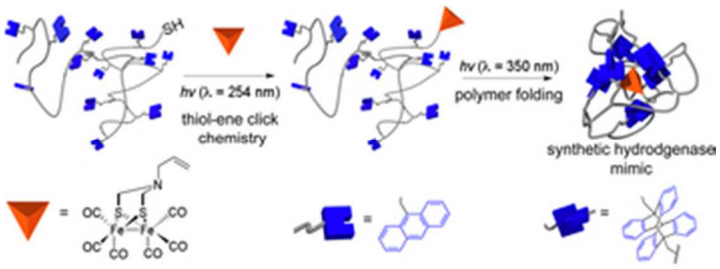

30x11mm (300 x 300 DPI)